4-2-2010

Effect of Surface Freezing on Meniscus Relaxation in Side Chain Comb Polymers

Shishir Prasad

Zhang Jiang

Michael Sprung

Sunil K. Sinha

Ali Dhinojwala
University of Akron Main Campus, ali4@uakron.edu

Effect of Surface Freezing on Meniscus Relaxation in Side Chain Comb Polymers

Shishir Prasad,[1] Zhang Jiang,[2] Michael Sprung,[3] Sunil K. Sinha,[2] and Ali Dhinojwala[1,*]

[1]*Department of Polymer Science, The University of Akron, Akron, Ohio 44325, USA*
[2]*Department of Physics, University of California San Diego, La Jolla, California 92093, USA*
[3]*Argonne National Laboratory, Chicago, Illinois 60439, USA*
(Received 20 July 2009; published 30 March 2010)

We have observed a sharp slowing down of the relaxation of the liquid meniscus for poly(n-alkyl acrylate) at temperatures where there are no abrupt changes in bulk viscosity or surface tension. This slowing down is due to the formation of a surface-ordered monolayer above the bulk melting temperatures. X-ray photon correlation spectroscopy measurements reveal that the surface capillary fluctuations are also significantly slower due to the formation of the ordered monolayer for film thicknesses comparable to that of the precursor films. The slowing down of the precursor film dynamics is responsible for slower meniscus relaxation below the surface ordering transition temperature.

The motion of the meniscus relaxation in poly(n-alkyl acrylate) (PA) liquid is slowed down considerably on cooling the liquid at temperatures where there are no abrupt changes in bulk viscosity or surface tension. This abrupt dynamic transition, at temperatures much higher than the bulk melting temperatures, cannot be explained by the traditional formalism used to describe the motion of liquid drops on solid surfaces. Typically, the spreading process of a liquid is divided into three regimes (based on the nomenclature by de Gennes [1]); flow in a macroscopic wedge, precursor film ahead of the wedge, and real contact line with the substrate [1–6]. The parameters such as viscosity, surface tension, and spreading coefficient determine the dynamics of spreading.

In this Letter, we have identified that the slowing down of the meniscus flow is due to the formation of an ordered monolayer on the surface of the PA melt. This 29 Å thick ordered monolayer on top of a disordered melt, measured using x-ray reflectivity, consists of all-trans hydrophobic alkyl side chains that undergo a first order-to-disorder transition at temperatures (T_s) 10–20 K above bulk melting temperature (T_m) [7–10]. The ordered layer slows down the capillary fluctuations, measured using x-ray photon correlation spectroscopy (XPCS), and has profound implications on the motion of the precursor film below T_s. It is intriguing that a 29 Å thin surface layer has such a dramatic influence on the dynamics of macroscopic contact line and has important technological implications in coating these materials at high speed and temperature above T_m.

Poly(octadecyl acrylate) [C18: $T_m = 320.7$ K, bulk freezing temperature (T_f) = 317.2 K, $T_{s,\text{heat}} = 329.8$ K, $T_{s,\text{cool}} = 328.3$ K] and poly(behenyl acrylate) [C22: $T_m = 336.5$ K, $T_f = 333.5$ K, $T_{s,\text{heat}} = 344.0$ K, $T_{s,\text{cool}} = 343.3$ K] were obtained from Landec Corp [9]. The T_s values were measured using multiple techniques and did not depend on the range of film thickness investigated in this study [11]. The polymers were synthesized using melt polymerization and had a $M_n \approx 15\,000$ g/mol and poly-

dispersity (PD) of ≈ 10. Meniscus relaxation experiments were performed using a Wilhelmy force balance and a thin platinum (Pt) wire of nominal diameter 0.5 mm (the actual diameter, $2r_0 = 0.53$ mm was calibrated using heptane). To avoid complications due to inertia, we have used conditions corresponding to low Bond numbers ($B_0 \approx 0.15 < 1$ [12]). Pt wire was cleaned using a flame torch just before starting the experiment. The experiments were also performed with a polystyrene (PS, $M_n = 1.03 \times 10^5$ g/mol, PD = 1.06, Polymer Source Inc.) coated Pt wire and a glass wire (diameter = 0.46 mm). We have conducted confirmatory experiments with polymers not exhibiting the surface freezing effect, polydimethylsiloxane (PDMS, $M_n = 2.0 \times 10^4$ g/mol, PD ≈ 6, Gelest Inc.). The polymer was placed in a temperature-regulated cell having a relative accuracy of 0.025 K and an absolute accuracy of 0.5 K. The wire was dipped into the polymer melt at a speed of 0.15 μm/sec and was stopped ≈ 300 μm inside the polymer melt. The force was measured as a function of time (time = 0 at instance when the wire became stationary). The time resolution in our force experiments is ≈ 1 sec. Static surface tension [$\gamma =$ (equilibrium force-buoyancy force)/(wire perimeter)] was measured by scanning the temperature at the rate of 0.1 K/min in steps of 0.2 K. The large surface energy of Pt metal ensures the equilibrium contact angle (θ_0) of the polymer to be $\approx 0°$. The error in absolute γ measurements is ± 0.5 mN/m.

The XPCS measurements were performed at the Advanced Photon Source (beam line 8-ID-I) at Argonne National Laboratory, using a synchrotron x-ray beam having energy of 7.35 keV. Thin films on silicon wafer for x-ray experiments were prepared by spin coating the polymer solution in toluene and subsequently annealing for overnight at 10 K above T_s. The thickness (h) of the films were measured using x-ray reflectivity. The incident angle of the beam was set at 0.14° (less than the critical angle for the total external reflection, 0.17°), to restrict the penetra-

tion depth of x-ray into the sample below the film thickness. The scattered intensity from the sample surface is collected using a direct-illumination CCD camera. Images taken at increasing time delays were analyzed to obtain the intensity autocorrelation function (g_2) as a function of the wave vector transfer parallel to the sample surface ($q_∥$). To confirm that there was no radiation damage, the data were only analyzed if the x-ray reflectivity measurements showed no differences before and after the XPCS measurements and we confirmed that the g_2's analyzed using different range of CCD images from a single set were identical.

The force relaxations for C18 and C22 above and below T_s are shown in Fig. 1. The relaxation dynamics are much slower below T_s ($\approx$4–6 hrs) compared to less than a second above T_s. The inset of Figs. 1(a) and 1(b) represent the static γ in heating cycle as a function of temperature for C18 and C22, respectively [9]. For static γ, the meniscus was equilibrated at $T > T_s$ for 2–3 h. The cell temperature was then changed in a cooling-heating cycle in steps of 0.2 K at 0.1 K/min and the data recorded after 10 min to ensure thermal equilibrium. The formation of the surface-ordered monolayer at T_s is marked by a sharp change in the slope of γ. The difference in the static γ values for these two temperature conditions (data shown in Fig. 1) is small ($<$0.8 mN/m). There is no dramatic change in viscosity at T_s and this slowing down cannot be explained by viscous effects. Therefore, the origin of the slowing down of the dynamics is due to formation of an ordered surface layer which results in a change in slope of surface tension [$d\gamma/dT = -(S_s - S_b)$, where S_s and S_b are entropy of the surface and the bulk, respectively] at T_s [9,13]. The

change in the sign of the slope indicates that the surface has a lower entropy than the bulk below T_s.

The late-stage recovery of the contact angle determined using the Wilhelmy balance also exhibits some unusual power laws below T_s [log-log plot for C18 and C22 in Figs. 2(a) and 2(b), respectively]. The values of θ_t were calculated using the measured force after correcting for the buoyancy. The steady state advancing contact angle for a substrate moving with a velocity U is given by $\theta \approx w^{0.33}$, where w is the capillary number $= U\eta/\gamma$ [1] and η is the viscosity of the liquid. When we stop the motion of the wire, the advancing contact angle will relax with time to its equilibrium value which in the case of Pt wire is $\theta = 0$, or complete wetting. The time $t = 0$ is defined when we stop the motion of the wire and the relaxation power laws we report here do not depend on the velocity or the immersion depth (discussed further in [11]). The solid lines in Figs. 2(a) and 2(b) are the power-law fits to the data indicating the power-law dependence of θ_t on t with exponent between -0.22 and -0.32. Using the no-slip boundary condition at air contact for $T_m < T < T_s$ [14], we obtain power-law exponent of -1.0 for triple contact line controlled and -0.5 for viscous dissipation in the wedge region dominated dynamics [1,6,11,15]. The same power law is expected for surface melt phase, and the two limits have been shown to hold both theoretically and experimentally for PDMS [5,6,16,17] and is clearly not observed for PA below T_s.

We can rule out other possibilities that could influence the power-law exponent. For example, the power-law exponent cannot be due to broad polydisperse PA samples
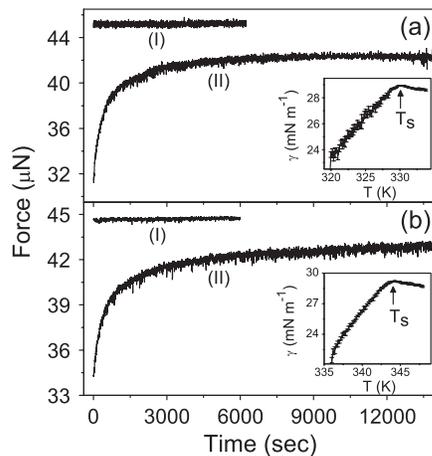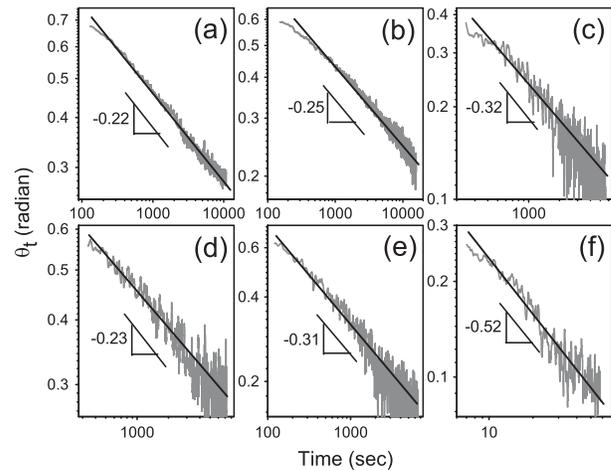

FIG. 1. The force experienced by the Pt wire during meniscus relaxation as a function of time for C18 (a) and C22 (b). The data are shown for $T > T_s$ (C18, 330.1 K; C22, 344.2 K) (I), and $T_m < T < T_s$ (C18, 328.0 K; C22, 342.7 K) (II). The insets represent the static γ of C18 (a) and C22 (b) measured in the heating cycles [9]. The arrows indicate T_s for the respective polymers. The meniscus relaxes within the experimental time resolution of 1 sec at $T > T_s$. In contrast, it relaxes over a period of 4–6 hr upon decreasing the temperature to $T < T_s$.

FIG. 2. θ_t during the late-stage meniscus relaxation process as a function of time in a log-log plot. The values are calculated using the force data as described in the text. The data are plotted for relaxation with a Pt wire of C18 at 328.0 K (a), C22 at 342.7 K (b), C18–C22 blend with 2 wt.% bulk concentration of C22 at 339.7 K (c). We have also plotted the relaxation of C18 at 328.0 K in contact with a glass wire (d), and a PS-coated Pt wire (e). The relaxation of PDMS with a Pt wire at 298.0 K is shown in (f). The solid lines are the power-law fits (the error of the fits were $\pm$0.01) to the data.

used in these experiments. Experiments on broad polydis-
perse PDMS [PD (~ 6)] shows a power-law exponent of
≈ 0.5 as expected for viscous dissipation [Fig. 2(f)]. A
similar power-law exponent was observed for glass wire
[Fig. 2(d)] and PS-coated Pt wire [Fig. 2(e)] confirming
that this is not due to substrate effects or spreading pa-
rameter. In addition, we have also measured PA blend of
2 wt. % C22 with C18 at temperatures above the T_m of C22
but below T_s [Fig. 2(c)]. In this blend, the surfaces are
expected to be covered with ordered monolayer of C22
molecules below the T_s transition temperature of C22 [18].
Not only do we observe the slowing down of the meniscus
dynamics at T_s corresponding to that of C22, but also the
power-law exponent is similar to that of pure C18 or C22.
All of these results confirm that we are observing here
slowing down of dynamics unlike that which has been
discussed before in the literature.

To understand the effect of a surface-ordered phase on
dynamics, we have performed XPCS measurements on
thin PA films of varying thickness supported on silicon
wafers. XPCS is an excellent technique to study the dy-
namics of small-scale surface height fluctuations. We ex-
pect capillary wave fluctuations to dominate the dynamics
of the precursor film, where the thicknesses of the film are
expected to be in the range from 100–200 Å [1,4,19,20].
For viscous liquids the slow capillary modes are strongly
overdamped and the relaxation times (τ) are determined by
the viscosity, surface tension, film thickness, and the wave
vector of the capillary waves [21]. The ratio of τ and
thickness (h) is proportional to the product of wave vector
($q_\parallel$) and h. The proportionality factor is related to the
viscosity/surface tension. For thin films, there is an addi-
tional dependence due to van der Waals interactions and
tethering of the chains with the substrate [11,22]. Fig-
ures 3(a)–3(c) and 3(d)–3(f) show g_2 at $q_\parallel = 1.65 \times 10^{-4}$ Å^{-1} for 220 and 660 Å thick C18 films, respectively.
The data are shown for bulk crystalline, surface-ordered,
and surface-melt phases. The capillary waves are frozen
below T_m and the values of g_2 are constant as expected
(speckle patterns are also provided in [11]). The formation
of the surface-ordered monolayer slows down the relaxa-
tion time of the capillary waves. The solid lines are fits
using a single-exponential function to determine τ [23].

The τ values as a function of $q_\parallel$ for four different
thicknesses above and below T_s are shown in Fig. 4. The
data for thick films (660 and 900 Å films) above T_s can be
modeled using the viscous model and the solid lines cor-
respond to a viscosity of 20 Pa s. This is in good agreement
with the viscosity measured using a parallel plate rheom-
eter ($\sim$20.6 Pa s). For thinner films (220 and 490 Å) the τ
values are higher than those predicted by the viscous
model, due to adsorption of the chains on the substrate,
and this effect is dominant when the thickness of the films
are comparable to the radius of gyration of the polymer
chains. The viscoelastic model which includes a shear
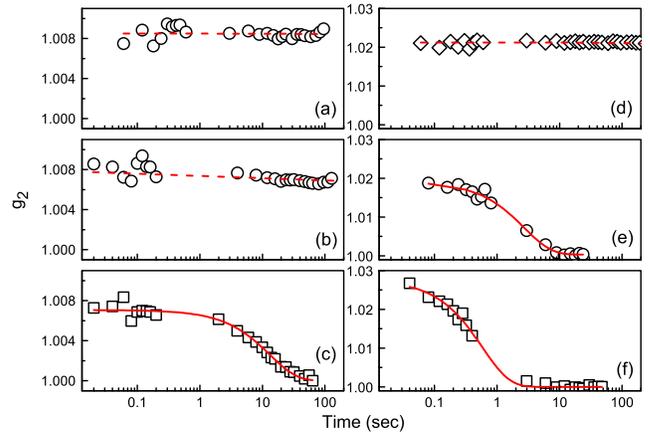modulus has been discussed before [22]. The data for

FIG. 3 (color online). Autocorrelation function (g_2) obtained
for C18 at $q_\parallel = 1.65 \times 10^{-4}$ Å^{-1} measured on 220 Å (a)–(c)
and 660 Å (d)–(f) thick films. The data are shown for $T < T_m$
(316.2 K) [(a),(d)], $T_m < T < T_s$ (327.2 K) [(b),(e)], and $T > T_s$
(331.2 K) [(c),(f)]. The solid lines are the single-exponential fits
to the data to obtain the relaxation time τ. The dashed lines are
the linear guides for the eye.

thinner films can be fitted using the viscoelastic model
and we obtain the shear modulus of 3–6 Pa and viscosity
between 90–130 Pa s. We were unable to determine more
exact values due to the small range of $q_\parallel$ accessible with
adequate signal-to-noise ratio.

In comparison, the surface fluctuations do not follow the
viscous model, even for thicker films, below T_s (at
327.2 K). The τ values determined using the viscous model
with $\eta = 24.3$ Pa s and $\gamma = 28$ mN/m are much lower
than those measured experimentally. The deviation is even
more striking for thinner films and the data cannot be
modeled by the viscoelastic model with a shear modulus
using the values determined above T_s. The formation of a
surface-ordered layer has dramatically slowed down the
capillary fluctuations. In fact, formation of this 29 Å thick
surface phase leads to the time independent g_2 at all $q_\parallel$ for
220 Å thick film with values above unity [Fig. 3(b) at $q_\parallel = 1.65 \times 10^{-4}$ Å^{-1}]. This indicates that quasistatic speckle
exists for long times, implying a very long relaxation time
in this temperature regime. We have also measured capil-
lary dynamics for 160 Å thin films and in that case, for both
above and below T_s, the values of g_2 are constant in the
time scale accessible by XPCS (determined by the beam
line stability, ≈ 8000 sec). Similar slowing down of dy-
namics for thin polystyrene films has also been observed
before when the film thicknesses are comparable to the
radius of gyration of the polymer chain [22]. For thicker
films, below T_s, we capture the slowing down of the
relaxation times by using a bilayer viscous model with
higher viscosity of the top layer [24]. However, the fits
are unacceptable for high $q_\parallel$ values. To explain the XPCS
data, in addition to the higher viscosity of the top layer, we
need to take into account the bending modulus of the
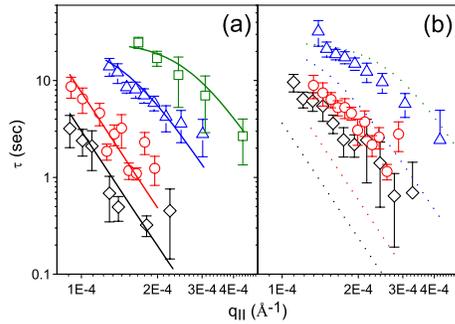surface-ordered layer. Buzza et al. [25] have taken into

FIG. 4 (color online).   The values of τ as a function of $q_{\parallel}$ for 220 ($\square$), 490 ($\triangle$), 660 ($\bigcirc$), and 900 ($\diamond$) Å thick C18 films at 331.2 K (a) and 327.2 K (b). The data for 220 Å thick film are not plotted at 327.2 K as time independent g_2 was observed (see text). The solid lines in (a) are the fits using the viscous model for 660 and 900 Å thick film and using viscoelastic model for 220 and 490 Å thick film (viscosity of 125 Pa s and shear modulus of 5 Pa). Shown as dotted lines in (b) are the calculated values of τ using the viscous model for 660 and 900 Å thick films and using a viscoelastic model for 220 and 490 Å thick films. We have taken into account the small differences in the bulk viscosity (3.6 Pa s) and surface tension (-0.7 mN/m [9]) between 331.2 K (above T_s) and 327.2 K (below T_s).

account the bending modulus of the surface surfactant layer. Sikharulidze *et al.* [26] have used the bulk bending modulus to explain their XPCS results for micron-thick smectic layers. However, none of these cases are for a rigid layer on top of a finite thickness liquid layer.

In summary, we have shown that the meniscus relaxation is slowed down dramatically after the formation of an ordered surface layer. The formation of a thin surface-ordered layer in the wedge region is not sufficient to slow down the dynamics. The power-law exponent for θ_t vs t below T_s[Figs. 2(a) and 2(b)] also does not match with the hypothesis that the wedge region or triple contact line is controlling the dynamics. Instead, we suggest that the meniscus relaxation is controlled by the motion of the 100–200 Å thick precursor film. This argument is supported by the XPCS data which unequivocally show that the formation of the surface-ordered layer considerably slows down the fluctuations of the capillary waves for films that are comparable to the thickness of the precursor films. We suggest that the bending rigidity and higher shear viscosity of the surface-ordered layer slows down the capillary fluctuations and the meniscus relaxation. The strong role of precursor film in controlling the meniscus dynamics is very intriguing considering that we expect only the spreading energy is burned in the precursor film [1]. The slowing down of wetting dynamics also has important commercial implications on the coatings of these polymers as release liners for pressure sensitive adhesives.

*ali4@uakron.edu
[1] P. G. de Gennes, Rev. Mod. Phys. **57**, 827 (1985).
[2] G. Inverarity, Br. Polym. J. **1**, 245 (1969).
[3] T. D. Blake and J. M. Haynes, J. Colloid Interface Sci. **30**, 421 (1969).
[4] D. Ausserre, A. M. Picard, and L. Leger, Phys. Rev. Lett. **57**, 2671 (1986).
[5] B. B. Sauer and W. G. Kampert, J. Colloid Interface Sci. **199**, 28 (1998).
[6] M.-J. Vega, D. Seveno, G. Lemaur, M.-H. Adao, and J. D. Coninck, Langmuir **21**, 9584 (2005).
[7] K. S. Gautam and A. Dhinojwala, Phys. Rev. Lett. **88**, 145501 (2002).
[8] K. S. Gautam, S. Kumar, D. Wermeille, D. Robinson, and A. Dhinojwala, Phys. Rev. Lett. **90**, 215501 (2003).
[9] S. Prasad, L. Hanne, and A. Dhinojwala, Macromolecules **38**, 2541 (2005).
[10] S. Prasad, Z. Jiang, S. K. Sinha, and A. Dhinojwala, Phys. Rev. Lett. **101**, 065505 (2008).
[11] See supplementary material at http://link.aps.org/supplemental/10.1103/PhysRevLett.104.137801 for surface transition temperatures, contact angle as a function of time, and models to analyze XPCS data.
[12] $B_0 = r_0/a$, where a is the capillary length given as $(\gamma/\rho g)^{1/2}$. γ is the surface tension of spreading liquid, ρ is the density of liquid, and g is the acceleration due to gravity [6].
[13] X. Z. Wu, B. M. Ocko, E. B. Sirota, S. K. Sinha, M. Deutsch, B. H. Cao, and M. W. Kim, Science **261**, 1018 (1993).
[14] P. Huber, V. P. Soprunyuk, J. P. Embs, C. Wagner, M. Deutsch, and S. Kumar, Phys. Rev. Lett. **94**, 184504 (2005).
[15] D. F. James, J. Fluid Mech. **63**, 657 (1974).
[16] D. Seveno and J. D. Coninck, Langmuir **20**, 737 (2004).
[17] D. Quere and J. M. Di Meglio, Adv. Colloid Interface Sci. **48**, 141 (1994).
[18] S. Prasad, L. Hanne, and A. Dhinojwala, Macromolecules **39**, 7467 (2006).
[19] A.-M. Cazabat, Contemp. Phys. **28**, 347 (1987).
[20] F. Brochard-Wyart, P. G. de Gennes, H. Hervert, and C. Redon, Langmuir **10**, 1566 (1994).
[21] H. Kim, A. Ruhm, L. B. Lurio, J. K. Basu, J. Lal, D. Lumma, S. G. J. Mochrie, and S. K. Sinha, Phys. Rev. Lett. **90**, 068302 (2003).
[22] Z. Jiang, H. Kim, X. Jiao, H. Lee, Y.-J. Lee, Y. Byun, S. Song, D. Eom, C. Li, and M. H. Rafailovich *et al.*, Phys. Rev. Lett. **98**, 227801 (2007).
[23] $g_2 = 1 + \beta \exp(-2t/\tau)$, where β is the speckle contrast [21].
[24] Z. Jiang, H. Kim, S. G. J. Mochrie, L. B. Lurio, and S. K. Sinha, Phys. Rev. E **74**, 011603 (2006).
[25] D. M. A. Buzza, J. L. Jones, T. C. B. McLeish, and R. W. Richards, J. Chem. Phys. **109**, 5008 (1998).
[26] I. Sikharulidze, B. Farago, I. P. Dolbnya, A. Madsen, and W. H. de Jeu, Phys. Rev. Lett. **91**, 165504 (2003).